

Morphology and preferred orientation of titanium nitride plates prepared by chemical vapour deposition

C. JIANG, T. GOTO, T. HIRAI

Institute for Materials Research, Tohoku University, Sendai 980, Japan

Thick titanium nitride (TiN_x ; $x = 0.74\text{--}1.0$) plates (up to 2 mm thick) were prepared by chemical vapour deposition using TiCl_4 , NH_3 and H_2 as source gases at a total gas pressure, P_{tot} , of 4 kPa, deposition temperatures, T_{dep} , from 1373–1873 K, and $\text{NH}_3/\text{TiCl}_4$, $m_{\text{N/Ti}}$, gas molar ratio from 0.17–1.74. The effects of deposition conditions on morphology, preferred orientation and composition of CVD- TiN_x plates were investigated. Surface morphology changed from faceted to nodular texture with increasing $m_{\text{N/Ti}}$ and T_{dep} . The faceted and nodular deposits showed columnar and shell-like fracture cross-sections, respectively. The composition ($x = \text{N/Ti}$) increased with increasing $m_{\text{N/Ti}}$ and T_{dep} below $m_{\text{N/Ti}} = 1.0$, and was constant above $m_{\text{N/Ti}} = 1.0$. Three kinds of preferred orientations were observed: (1 0 0) orientation at low T_{dep} , (1 1 0) orientation at intermediate T_{dep} and low $m_{\text{N/Ti}}$, and (1 1 1) orientation at high T_{dep} and high $m_{\text{N/Ti}}$. This tendency is discussed thermodynamically, and explained as being due to changes in the degree of supersaturation in the gas phase.

1. Introduction

Titanium nitride film is widely used as a coating material due to its high melting point, hardness and good erosion/corrosion resistance [1]. However, the intrinsic properties of TiN_x film are not well understood because such film prepared by physical vapour deposition (PVD) [2–5] or chemical vapour deposition (CVD) [3, 6–9] are usually too thin to measure many properties. Therefore, it is necessary to prepare massive, highly pure TiN_x plates to investigate the relationship between intrinsic properties and microstructures of TiN_x .

CVD is one of the most suitable techniques for preparing high-purity materials. So far, no papers have been published on the preparation of CVD- TiN_x plates with a thickness of more than 1 mm. Until now, CVD- TiN_x film has been prepared mainly using the $\text{TiCl}_4 + \text{N}_2 + \text{H}_2$ system. Nearly all the papers have reported that deposition rates were about several micrometres per hour and that the thickness ranged from several tens to several hundreds of micrometres [6–12].

We prepared thick plates of CVD- Si_3N_4 [13], CVD- AlN [14], CVD- BN [15], etc., at high deposition rates of around 1 mm h^{-1} using a combination of a cold-wall type CVD reactor, a nozzle with double tubes for blowing gas and ammonia gas as a nitrogen source due to its high reactivity. In the present work, thick (up to 2 mm) CVD- TiN_x plates were prepared by using the above-mentioned technique at high deposition rates (about 0.4 mm h^{-1} maximum).

In this study, the optimum CVD conditions for the preparation of TiN_x thick plates in the $\text{TiCl}_4 + \text{NH}_3 + \text{H}_2$ system were investigated. The effects of

deposition conditions on surface texture, composition and preferred orientation for CVD- TiN_x plates were also studied.

2. Experimental procedure

Fig. 1 shows a schematic diagram of the CVD apparatus used. TiCl_4 liquid (99.99%), NH_3 gas (99.9%) and hydrogen gas (99.999%) were used as source materials. The TiCl_4 liquid was bubbled by hydrogen gas and the TiCl_4 vapour was introduced into a cold-wall reactor through a quartz nozzle with double tubes. NH_3 and $\text{TiCl}_4 + \text{H}_2$ were separately introduced into the reaction chamber to reduce the formation of NH_4Cl powder. Graphite substrates were heated by transmission of an electric current. TiCl_4 and H_2 gas flow rates were both fixed at constant values. The molar ratio TiCl_4 to NH_3 ($m_{\text{N/Ti}}$) was changed by controlling the NH_3 gas flow rate. Deposition temperatures, T_{dep} , were varied in the range 1373–1873 K. Total gas pressure, P_{tot} , was kept at 4 kPa. Above $P_{\text{tot}} = 4 \text{ kPa}$, the deposition temperature could not be measured precisely with a two-colour pyrometer owing to the large amount of NH_4Cl powder formed in the gas phase. The deposition conditions are summarized in Table I.

Surface textures were examined by a scanning electron microscope (SEM). Compositions were determined by inductively coupled plasma analysis (ICP) and electron-probe microanalysis (EPMA). Preferred orientation was studied by a X-ray diffractometer (nickel-filtered, CuK_α). Lattice parameters, non-stoichiometry and the deposition mechanism have been reported elsewhere [16].

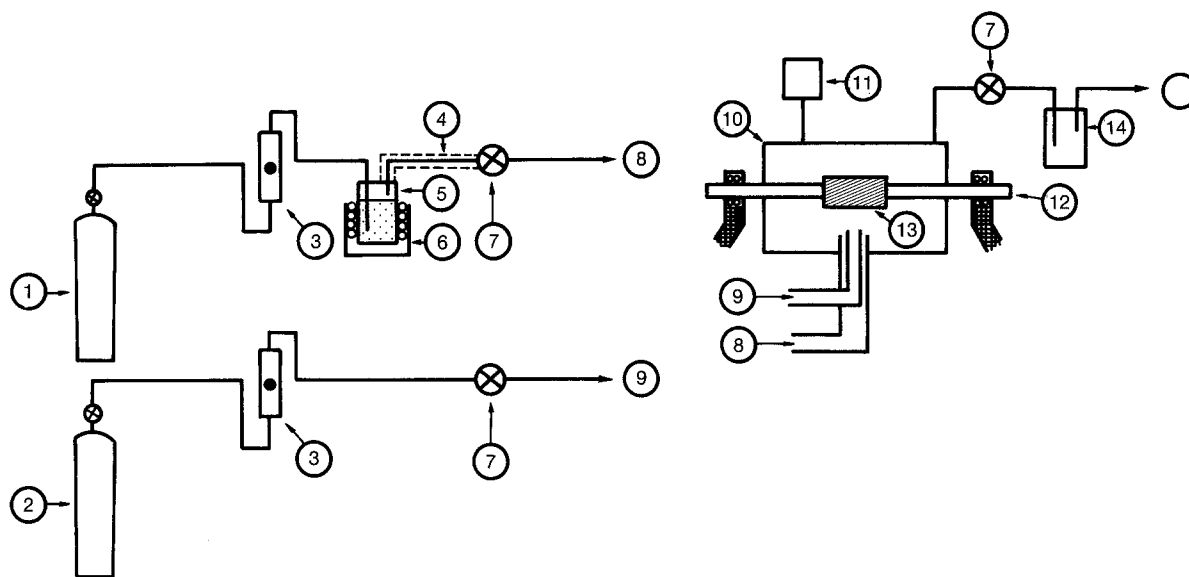


Figure 1 Schematic diagram of the CVD apparatus: (1) H₂ gas, (2) NH₃ gas, (3) gas flow meter, (4) ribbon heater, (5) TiCl₄ reservoir, (6) constant temperature bath, (7) valve, (8) TiCl₄ + H₂ gases inlet, (9) NH₃ gas inlet, (10) reaction chamber, (11) pressure indicator, (12) copper electrode, (13) graphite substrate, (14) cold trap, (15) rotary pump.

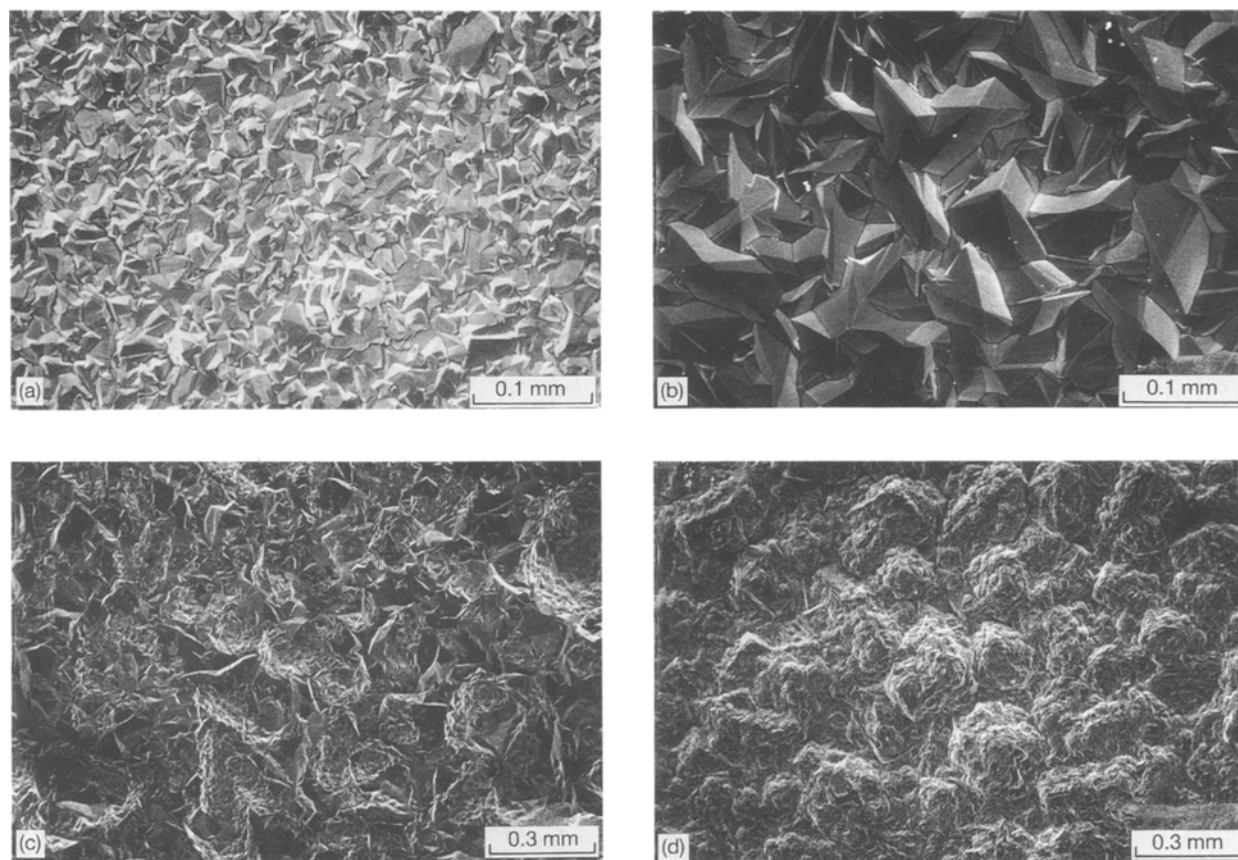


Figure 2 Relationship between surface texture and $m_{N/Ti}$ for the CVD-TiN_x plates prepared at (a) $m_{N/Ti} = 0.17$, (b) $m_{N/Ti} = 1.04$, (c) $m_{N/Ti} = 1.30$ and (d) $m_{N/Ti} = 1.74$. ($T_{dep} = 1573$ K)

3. Results and discussion

3.1. Microstructure

Fig. 2 shows the relationship between surface texture and $m_{N/Ti}$ of the CVD-TiN_x plates prepared at $T_{dep} = 1573$ K. The faceted and nodular deposits were obtained below and above $m_{N/Ti} = 1.3$, respectively.

The morphology of surface texture mainly depended on $m_{N/Ti}$. The relationship between surface texture and deposition conditions is depicted in Fig. 3. The present results are in agreement with the general trend in findings that the surface texture tends to change from facet to nodule with increasing $m_{X/M}$, in which X rep-

TABLE I Deposition conditions

Deposition temperature, T_{dep} (K)	1373–1873
Total gas pressure, P_{tot} (kPa)	4
Gas flow rate, FR ($\text{m}^3 \text{s}^{-1}$)	
$FR(\text{H}_2)$	3.4×10^{-5}
$FR(\text{TiCl}_4)$	1.9×10^{-6}
$FR(\text{NH}_3)$	0.3×10^{-6} – 3.3×10^{-6}
$\text{NH}_3/\text{TiCl}_4$, $m_{\text{N/Ti}}$	0.17–1.74
Deposition time, t (ks)	7.2–21.6

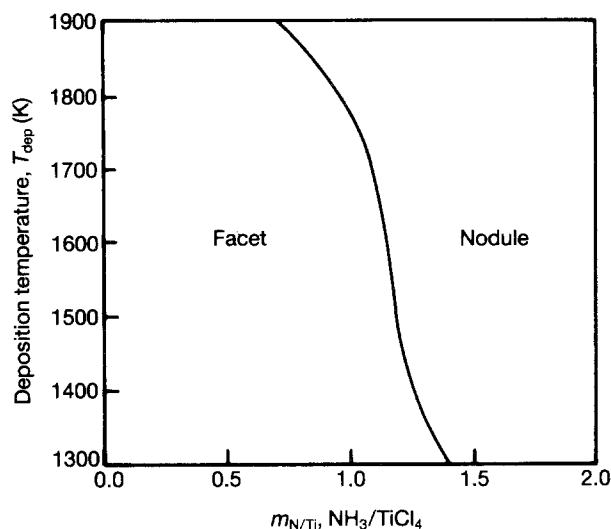


Figure 3 Relationship between surface texture and deposition conditions.

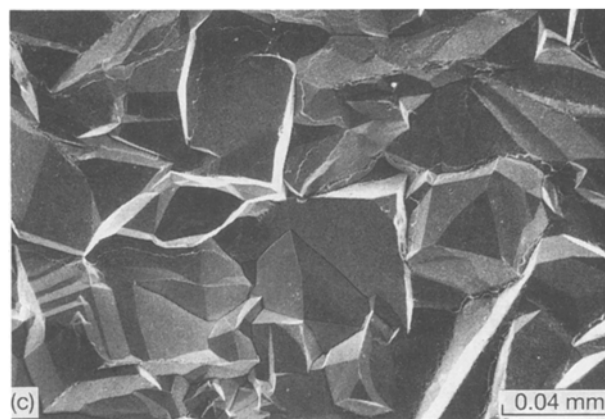
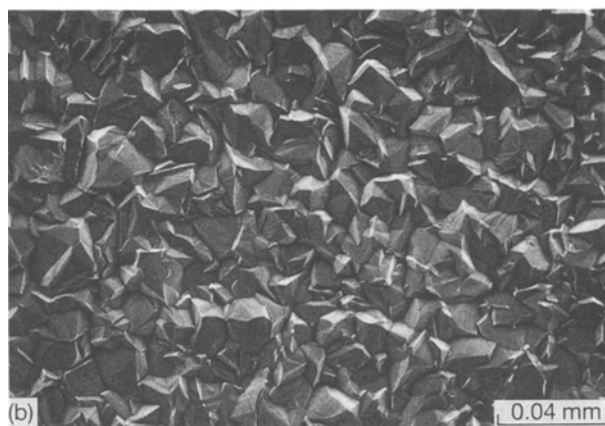
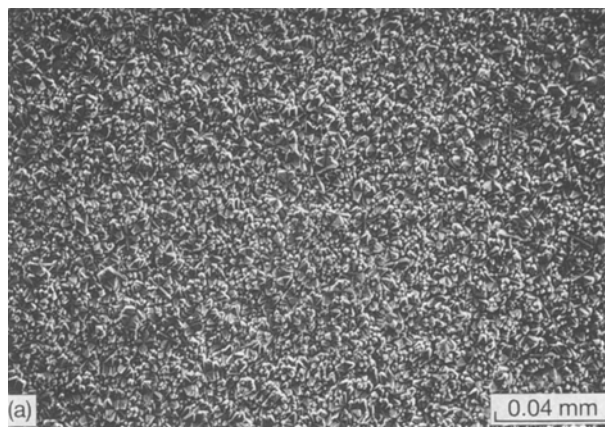
resents non-metal elements such as nitrogen, carbon, etc. and M is metal elements such as aluminium, silicon etc., as reported for CVD–AlN [14] and CVD–SiC [17] plates.

Fig. 4 demonstrates the effect of deposition temperature, T_{dep} , on surface texture of the CVD–TiN_x plates prepared at $m_{\text{N/Ti}} = 0.17$. All deposits show the faceted texture, and the grain size increased from 3 μm to 40 μm with increasing T_{dep} . On the other hand, the grain size of nodular deposits was almost independent of T_{dep} .

Fig. 5a and b show the fractured cross-sectional surface of faceted and nodular deposits, respectively. The faceted deposits have a clear columnar structure, while the nodular deposits have a shell-like fracture surface. This result is in agreement with those reported for CVD–Si₃N₄ [13] and CVD–SiC plates [17]. The grain size near the substrate is very much smaller than that near the surface in both types of deposit.

3.2. Composition

Fig. 6 shows the relationship between composition, x ($x = \text{N/Ti}$) and $m_{\text{N/Ti}}$. Nitrogen-deficient non-stoichiometric CVD–TiN_x ($x < 1$) plates were obtained below $m_{\text{N/Ti}} = 1.0$, and stoichiometric CVD–TiN_x ($x = 1$) plates were obtained above $m_{\text{N/Ti}} = 1.0$. The composition, x , increased with increasing $m_{\text{N/Ti}}$ and T_{dep} below $m_{\text{N/Ti}} = 1.0$, and x was independent of $m_{\text{N/Ti}}$ and T_{dep} above $m_{\text{N/Ti}} = 1.0$. Teysandier *et al.* [9] prepared CVD–TiN_x films using the

Figure 4 Effect of deposition temperature, T_{dep} , on surface texture of CVD–TiN_x plates prepared at T_{dep} (a) 1373 K, (b) 1573 K and (c) 1773 K. ($m_{\text{N/Ti}} = 0.17$)

TiCl₄ + N₂ + H₂ system at $T_{\text{dep}} = 1200$ – 1400 K and $m_{\text{N/Ti}} = 0.25$ – 10 , and calculated their composition, x , to be in the range 0.63– 1.0 by measuring lattice parameters. They reported that stoichiometric TiN_x films could be prepared at atmospheric pressure ($P_{\text{tot}} = 0.1$ MPa) and non-stoichiometric films ($x < 1$) at reduced pressure ($P_{\text{tot}} = 0.7$ kPa).

However, in the present work, both stoichiometric and non-stoichiometric CVD–TiN_x plates were obtained by using the TiCl₄ + NH₃ + H₂ system at reduced pressure ($P_{\text{tot}} = 4$ kPa). This difference seems to be the result of the higher reactivity of ammonia as compared with that of nitrogen gas.

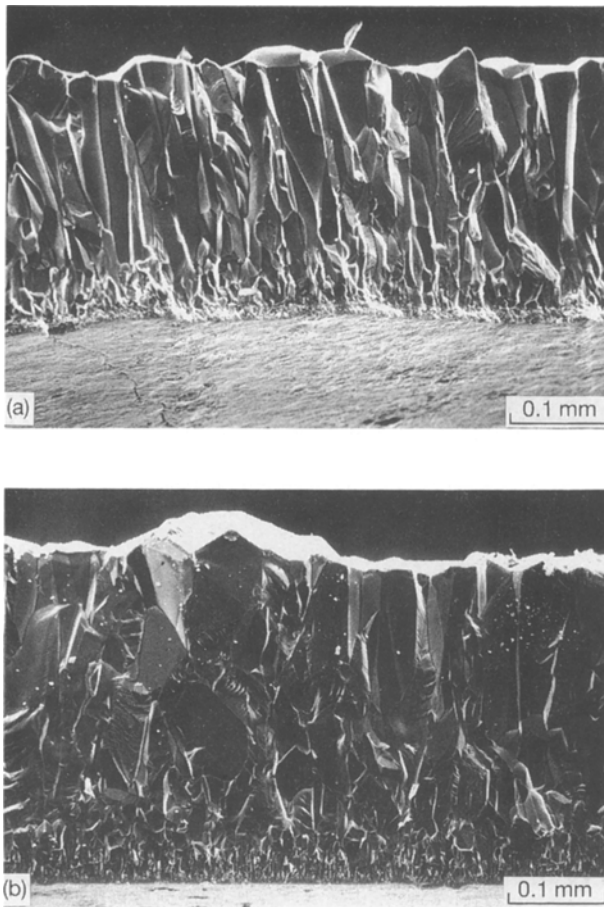


Figure 5 Cross-sectional fracture surface. (a) Faceted deposit prepared at $m_{N/Ti} = 0.17$ and $T_{dep} = 1673$ K, (b) nodular deposit prepared at $m_{N/Ti} = 1.74$ and $T_{dep} = 1573$ K.

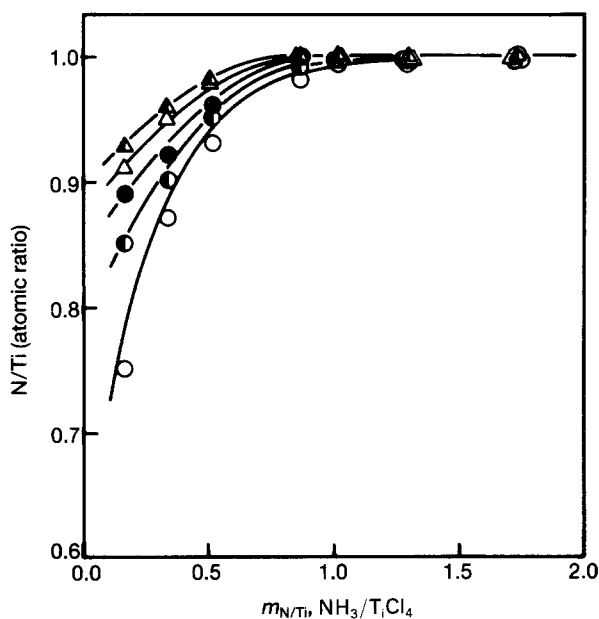


Figure 6 Relationship between composition, x , of CVD-TiN_x plates and $m_{N/Ti}$. T_{dep} (K): (\blacktriangle) 1873, (\triangle) 1773, (\bullet) 1573, (\circ) 1473, (\circ) 1373.

3.3. Preferred orientation

Fig. 7 shows typical X-ray diffraction patterns of oriented CVD-TiN_x plates. Three kinds of preferred orientations, i.e. (100), (110) or (111) orientations, were observed.

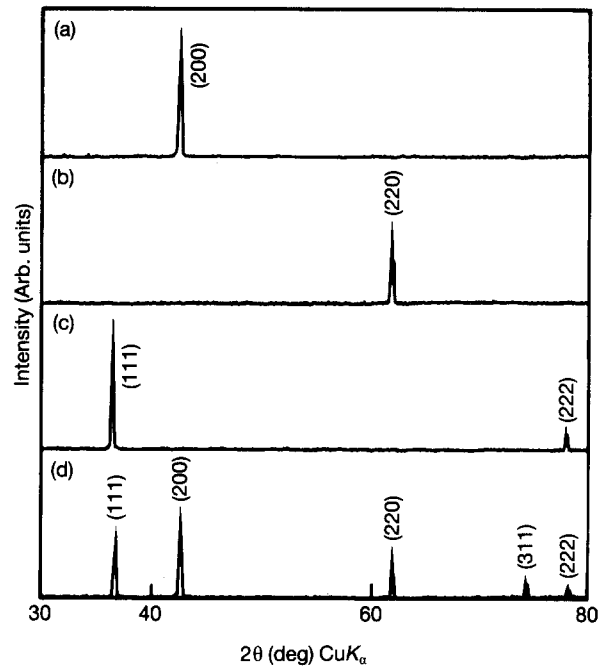


Figure 7 Typical X-ray diffraction patterns of oriented CVD-TiN_x plates prepared at (a) $T_{dep} = 1373$ K and $m_{N/Ti} = 0.87$, (b) $T_{dep} = 1673$ K and $m_{N/Ti} = 0.17$, and (c) $T_{dep} = 1573$ K and $m_{N/Ti} = 0.87$; (d) powder pattern.

Fig. 8 shows the surface texture of typically oriented CVD-TiN_x plates. The surface texture was closely related to the preferred orientation. Fig. 9 may explain each orientation by illustrating the shape of the unit cell. The hatched areas in the figures are parallel to the substrate. In the (100) orientated deposits, see Fig. 8a, many cubic grains which correspond to Fig. 9a, are easily detected. In the (110) orientated deposits, see Fig. 8b, the surface is covered with inclined facets which are similar to that shown in Fig. 9b. In the (111) orientated deposits, see Fig. 8c, many triangles can be seen as illustrated in Fig. 9c.

The preferred orientation of the specific (hkl) plane can be evaluated by texture coefficient, $TC(hkl)$. [7, 18]

$$TC(hkl) = \frac{I_m(hkl)}{I_r(hkl)} \bigg/ \frac{1}{n} \sum_{i=1}^n \frac{I_m(hkl)}{I_r(hkl)} \quad (1)$$

where $I_m(hkl)$ is the measured X-ray relative intensity of the (hkl) plane, $I_r(hkl)$ is the relative intensity in the powder pattern, and n is the total number of reflection peaks. The larger TC values mean a more remarkable orientation. If $TC(hkl)$ is less than 1, the (hkl) plane has no preferred orientation.

Fig. 10 depicts the effect of deposition temperature, T_{dep} , on preferred orientation of (100), (110) and (111) at $m_{N/Ti} = 0.34$. The preferred orientation changes from (100) to (110) to (111) with increasing T_{dep} . The maximum TC values were about 4 for each orientation. The relationship between preferred orientation and CVD conditions is demonstrated in Fig. 11. The (100) orientation was dominant at low T_{dep} , the (111) orientation was significant at high T_{dep} and high $m_{N/Ti}$, and the (110) orientation was observed at intermediate T_{dep} and low $m_{N/Ti}$.

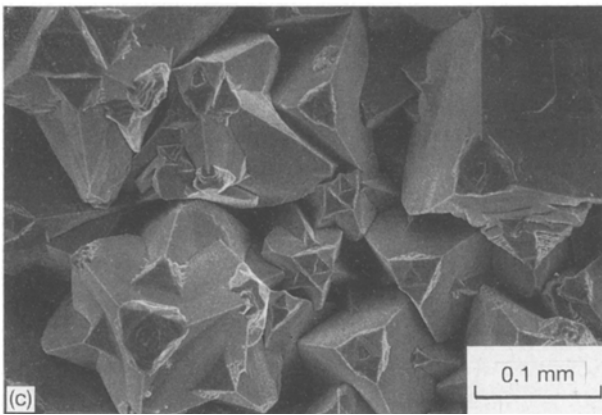
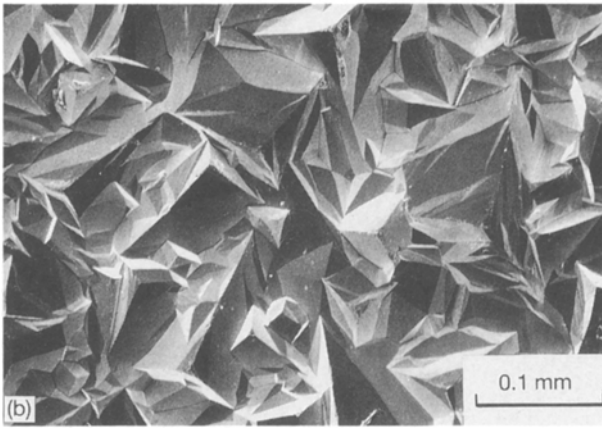
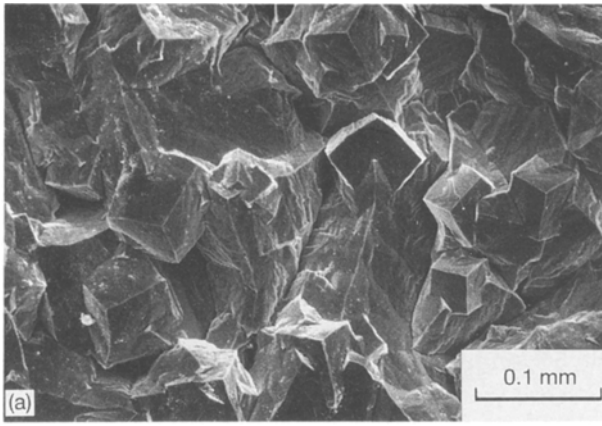


Figure 8 Typical surface texture of oriented CVD-TiN_x plates. (a) (100) orientation: $T_{\text{dep}} = 1373$ K and $m_{\text{N/Ti}} = 0.87$. (b) (110) orientation: $T_{\text{dep}} = 1673$ K and $m_{\text{N/Ti}} = 0.17$. (c) (111) orientation: $T_{\text{dep}} = 1573$ K and $m_{\text{N/Ti}} = 0.87$.

Takahashi and Suzuki [11] reported that CVD-TiN_x films prepared on graphite substrates had no orientation in the T_{dep} range between 973 and 1273 K, the (100) orientation at $T_{\text{dep}} = 1373$ K and the (110) orientation above $T_{\text{dep}} = 1473$ K. Sadahiro *et al.* [10] showed that CVD-TiN_x films on WC-6%Co substrates had the (110) orientation at $T_{\text{dep}} = 1273$ –1373 K. Kim and Chun [7] also indicated that CVD-TiN_x films on WC-6%Co substrates had the (100) orientation at $T_{\text{dep}} = 1223$ –1273 K and the (110) orientation at $T_{\text{dep}} = 1373$ –1423 K. There is a trend that the preferred orientation of CVD-TiN_x changes from (100) to (110) to (111) with increasing T_{dep} . This trend is consistent with the present work, as shown in

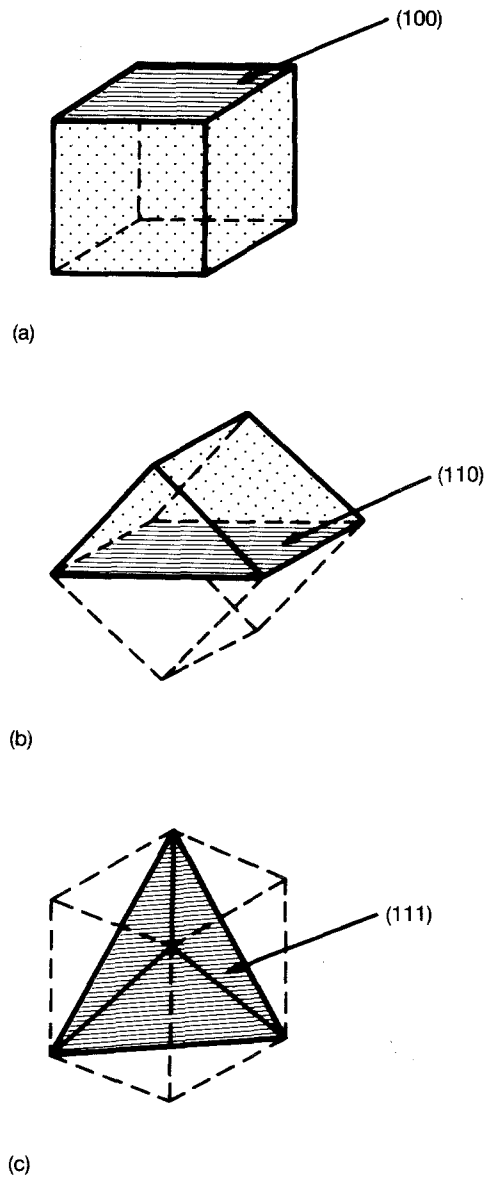


Figure 9 Morphological aspects of TiN_x. (a) (100) orientation, (b) (110) orientation, (c) (111) orientation.

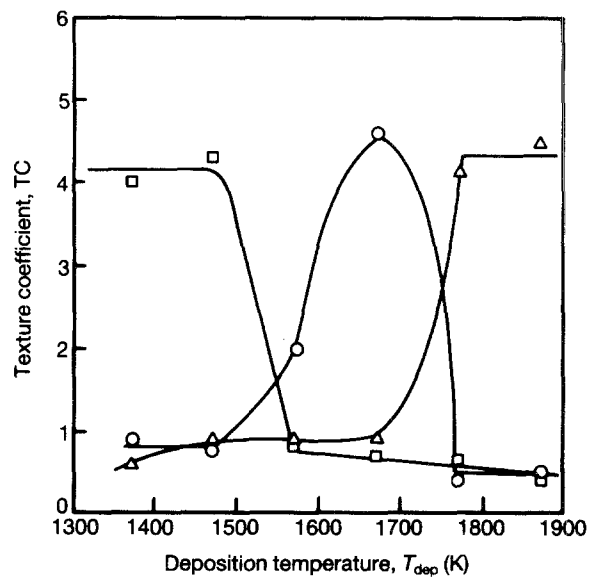


Figure 10 Effect of deposition temperature, T_{dep} , on texture coefficient, TC. (□) (100), (○) (110), (△) (111).

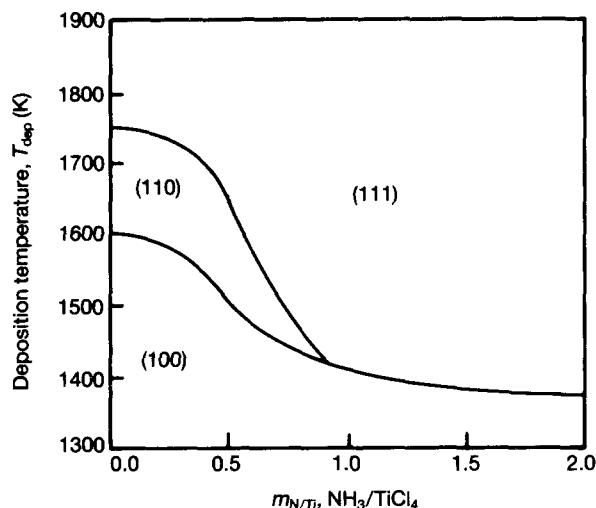


Figure 11 Relationship between the preferred orientation of CVD-TiN_x plates and deposition conditions.

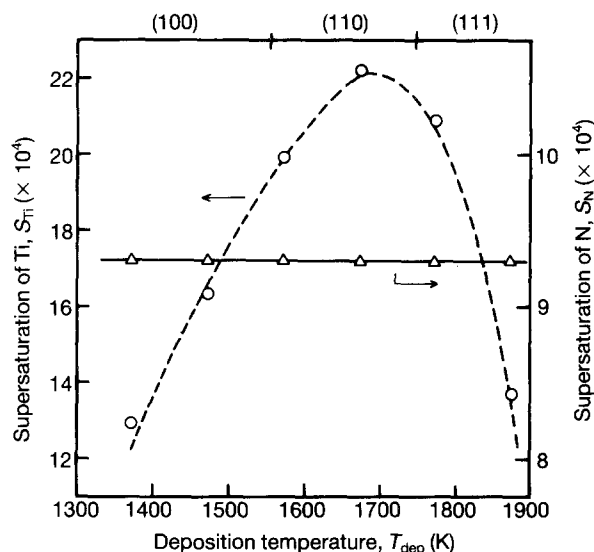


Figure 12 Effect of deposition temperature, T_{dep} , on supersaturation. (○) S_{Ti} , (△) S_N .

Fig. 10. However, there have been no reports published on the reason for the preferred orientation of CVD-TiN_x film.

Pangarov [19] proposed a model which might explain the relationship between orientation of electro-deposited metals and supersaturation in a solution: it may possibly explain the preferred orientation of CVD materials as reported for CVD-AlN [14] and CVD-TiB₂ plates [20]. According to the calculation by Pangarov [19], the preferred orientation of TiN_x could be changed from (111) to (100) to (110) with increasing supersaturation. The supersaturation, S , in the CVD process may be defined as

$$S_i = n P^{in}(i) / \sum_j n_j P_j^{eq}(i) \quad (2)$$

where S_i is the supersaturation of i species and $P^{in}(i)$ is the partial pressure of i species in the source gas. P_j^{eq} was calculated by the computer code SOLGAS-MIX-PV [21] using thermochemical data [22] of gas

species in the Ti-N-H-Cl system. Fig. 12 shows the temperature dependence of the supersaturation of titanium-containing species, S_{Ti} , and nitrogen-containing species, S_N . S_N is almost independent of T_{dep} , but S_{Ti} has a maximum at about $T_{dep} = 1700$ K. Although the calculated S_{Ti} above $T_{dep} = 1800$ K is almost similar to that below $T_{dep} = 1500$ K, it is likely that the actual S_{Ti} above $T_{dep} = 1800$ K is much smaller than the calculated value due to a large amount of powder formation. Therefore, the variation of preferred orientation with T_{dep} may be explained by the change in supersaturation.

4. Conclusions

Titanium nitride plates up to 2 mm thick were prepared by CVD using TiCl₄, NH₃ and H₂ as source gases under the following conditions: $T_{dep} = 1373$ – 1873 K, $P_{tot} = 4$ kPa, and $m_{N/Ti} = 0.17$ – 1.74 . The following results were obtained.

1. The surface texture changed from faceted to nodular texture with increasing $m_{N/Ti}$ and T_{dep} .
2. The non-stoichiometry of CVD-TiN_x was controlled from $x = 0.74$ – 1.0 by changing T_{dep} and $m_{N/Ti}$. The x value increased with increasing T_{dep} and $m_{N/Ti}$ below $m_{N/Ti} = 1.0$, and was constant above $m_{N/Ti} = 1.0$.
3. There were three kinds of preferred orientation depending on the CVD conditions: (100) orientation at low T_{dep} , (110) orientation at intermediate T_{dep} and low $m_{N/Ti}$, and (111) orientation at high T_{dep} and high $m_{N/Ti}$. The relationship between preferred orientation and CVD conditions was explained as being due to the change of supersaturation in the gas phase.

Acknowledgements

The authors thank Mr T. Narushima for ICP analysis and Mr F. Wagatsuma for EPMA analysis. This research was supported in part by the Grant-in-Aid for Scientific Research from the Ministry of Education, Science and Culture under Contracts 02203105 and 63850149.

References

1. D. P. STINTON, T. M. BESMANN and R. A. LOWDEN, *Am. Ceram. Soc. Bull.* **67** (1988) 350.
2. J. E. SUNDGREN, *Thin Solid Films* **128** (1985) 21.
3. K. H. HABIG, *J. Vac. Sci. Technol.* **A4** (1986) 2832.
4. P. J. BURNETT and D. S. RICKERBY, *J. Mater. Sci.* **23** (1988) 2429.
5. W. D. SPROUL, *J. Vac. Sci. Technol.* **A4** (1986) 2874.
6. J. S. CHO, S. W. NAM and J. S. CHUN, *J. Mater. Sci.* **17** (1982) 2495.
7. M. S. KIM and J. S. CHUN, *Thin Solid Films* **107** (1983) 129.
8. C. H. J. VAN DEN BREKEL, R. M. M. FONVILLE, P. J. M. VAN DER STRATEN and G. VERSPUI, in "Proceedings of the 8th International Conference on Chemical Vapour Deposition", edited by J. M. Blocher, J. Wahl and G. E. Vuillard (Electrochemical Society, Princeton, NJ, 1981) p. 142.
9. F. TEYSSANDIER, C. BERNARD and M. DUCARROIR, in "Proceedings of the 6th European Conference on Chemical Vapor Deposition", edited by R. Porat (Iscar, Jerusalem, 1987) p. 96.

10. T. SADAHIRO, T. CHO and S. YAMAYA, *J. Jpn Inst. Metals* **41** (1977) 542.
11. T. TAKAHASHI and Y. SUZUKI, *Nippon Kagaku Kaisi* **6** (1974) 1043.
12. T. TAKAHASHI and H. ITOH, *J. Electrochem. Soc.* **124** (1977) 797.
13. K. NIIHARA and T. HIRAI, *J. Mater. Sci.* **11** (1976) 593.
14. T. GOTO, J. TSUNEYOSHI, K. KAYA and T. HIRAI, *J. Mater. Sci.* **27** (1992) 247.
15. T. MATSUDA, N. UNO, H. NAKAE and T. HIRAI, *ibid.* **21** (1986) 649.
16. C. JIANG, T. GOTO and T. HIRAI, to be published in *J. Mater. Sci.*
17. T. HIRAI, T. GOTO and T. KAJI, *Yogyo-Kyokai-Shi* **91** (1983) 502.
18. C. S. BARRETT and T. B. MASSALAKI, in "Structure of Metals" (Pergamon, Oxford, 1980) p. 205.
19. N. A. PANGAROV, *Electrochim. Acta* **9** (1964) 721.
20. M. MUKAIDA, T. GOTO and T. HIRAI, *J. Mater. Sci.* **26** (1991) 6613.
21. T. M. BESMANN, Oakridge National Laboratory Technical Report ORNL/TM-5775 (April, 1975).
22. D. R. STULL and H. PROPHET (eds), "JANAF Thermochemical Tables", 2nd Edn, NSRDS-NMS-37 (US Government Printing Office, Washington, DC, 1971).

*Received 9 June 1992
and accepted 9 August 1993*